Object-based 3D damage assessment using surface models derived from mixed-date stereo models

Sebastian d'Oleire-Oltmanns[1], Dirk Tiede[1], Thomas Krauß[2], Lorenz Wendt[1]

1. Department of Geoinformatics - Z_GIS, University of Salzburg
Schillerstr. 30, 5020 Salzburg, Austria
sebastian.doleire-oltmanns@sbg.ac.at

2. German Aerospace Center (Deutsches Zentrum für Luft- und Raumfahrt; DLR
Oberpfaffenhofen, 82234 Weßling, Germany

ABSTRACT. Damage assessment is a crucial aspect in different scientific but also publicly relevant fields. Especially in the humanitarian context the estimation is often time critical as conflict events, but also natural disasters urge a quick response. The presented approach analyzes the potential of cross-stereo satellite imagery, i.e. images from different dates of the same or even different satellite sensors, to allow the generation of pre- and post-event 3D information. The study area is located in the city of Mosul, Iraq. The concept of object-based analysis was applied for the 3D damage assessment. The classification outcomes are categorized in four different height classes. 73 % of the point reference data matches with the classification results of the damage assessment.

KEYWORDS: cross-stereo models, digital surface models, damage assessment, mixed data stereo models, 3D change detection

1. Introduction

The usage of 2D image information and 3D terrain information for investigating numerous environments has been conducted within various applications: Structural biodiversity monitoring in savanna ecosystems (Levick & Rogers, 2008), the integrated analysis of 2D and 3D data sets such as airborne laser scanning data for building detection (Rutzinger *et al.*, 2008), data fusion of objects for cultural heritage applications (Serna *et al.*, 2015), and measuring soil erosion in different extents (d'Oleire-Oltmanns *et al.*, 2012; Stöcker *et al.*, 2015). The assessments or change detections were carried out on different spatial extents, from small-scale surface reconstruction (Kaiser *et al.*, 2014) to mapping grassland habitat distribution at local and regional scales *(Buck et al.*, 2014) to landform mapping at multiple scales (d'Oleire-Oltmanns *et al.*, 2012). One main advantage of digital information in 2D and 3D is the possibility to cover areas that are either very large or hardly accessible, maybe even both (Strasser & Lang, 2015; Symeonakis & Drake, 2004; Vrieling et al., 2007).

Damage assessment is a crucial aspect in different scientific but also publicly relevant fields. For urban contexts, different approaches have been carried out using VHR optical and SAR imagery (Brunner *et al.*, 2010). It is of particular interest after earthquakes (Kosugi *et al.*, 2004). An overview to rapid assessment of earthquake damage has been published by Erdik *et al.*, (2011). The availability of 3D elevation information is able to improve the assessments based on 2D image data only, especially in estimating the magnitude of damaged buildings.

Especially in the humanitarian context the estimation is often time critical as conflict events, but also natural disasters urge a quick response from e.g. international non-governmental organizations (NGO). Hence, the assessment is supposed to be quick, reliable as well as covering best possibly the whole area of investigation, whereas the accuracy is set second priority. This may be carried out based on damage indication for rapid geospatial reporting (Tiede *et al.*, 2011).

Another aspect is the availability and pricing of the 3D data required for the analysis. The approach presented here is part of the ongoing research project X3D4Pop, which analyzes the potential of cross-stereo satellite imagery, i.e. images from different dates of the same or even different satellite sensors, to allow the generation of pre and post-event 3D information also in data-scarce situations. This 3D information may be used for change detection, damage assessment, and even population estimation based on building height derivation.

2. Study area and data used

2.1 Study area and context

The study area is located in the city of Mosul in the Ninawa Governate of Iraq, approximately 400 km north of Bagdad (see FIGURE 1). The city was attacked and conquered by the "Islamic State" militia (IS) in June 2014 together with extensive areas of surrounding territory. In October 2016 a coalition led by the Iraqi army launched a counter offensive, during which the IS militia pulled back into the old town of Mosul. After bombardment and heavy shelling, the entire city could be recaptured in July 2017. The old town, as the last refuge of the IS militants, was heavily damaged in the process (BBC 2017, online).

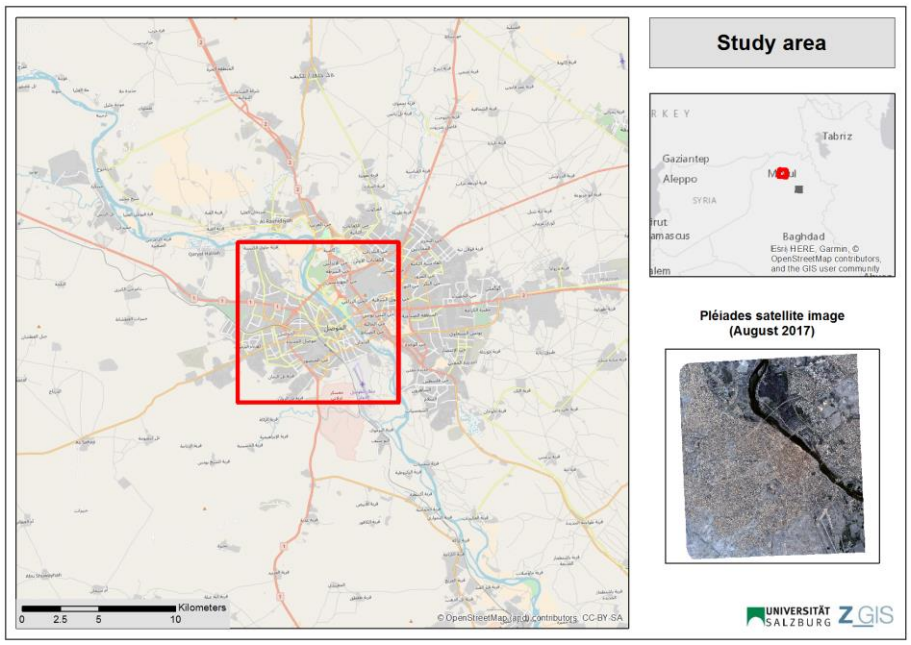

FIGURE 1. Study area as defined for this work is the city of Mossul. Illustrations based on ESRI Basemaps, OpenStreetMap and Pléiades satellite imagery.

2.2 Satellite data used for DSM generation

The investigation is based on Pléiades data from 2015-05-06, 2017-08-21 and 2017-09-04. The first dataset is a stereo-triple dataset containing three pan-chromatic and three multispectral images acquired 2015-05-06 from PHR-1B at 08:00:18.4 UTC (pan-chromatic image referred as d), 07:59:39.1 UTC (e) and

08:00:04.5 UTC (f). The second dataset are single satellite images consisting of a pan-chromatic and multispectral image each acquired by PHR-1A at 2017-08-21, 08:04:17.8 UTC (h) and 2017-09-04, 07:56:37.8 (j) respectively. The illumination change is only 0.5 degree during the 2015-triple acquisition and 5.4 degree between the two individual images from 2017. The satellite imagery provides a per-pixel spatial resolution of 0.5 m x 0.5 m and the derived DSM datasets also provide a per-pixel spatial resolution of 0.5 m x 0.5 m.

TABLE 1. Convergence angles between selected pan-chromatic images.

Acquisition Date(s)	Image pair	Angle
06 May 2015	d-e	1.38°
	d-f	7.05°
	e-f	8.41°
21 Aug 2017/ 04 Sep 2017	h-j	11.86°

2.3 Reference data

An independent visual damage assessment of the Old Town of Mosul conducted by UNOSAT (UNOSAT, 2017), based on a WorldView-3 very-high resolution satellite image of 18. July 2017, was available as reference data set. Damages were categorized into three categories: “Destroyed”, “Severe damage” and “Moderate damage”, and marked with a point marker. Undamaged or only slightly damaged buildings were not marked. In total, 6,981 affected structures were mapped in this part of the city. Due to the dense building structure in the old town, these numbers are reported to be potentially underestimated. Damages were not validated in the field (UNOSAT, 2017). Damage assessment maps and vector data are available for download. The area covered with reference data is illustrated in FIGURE 2.

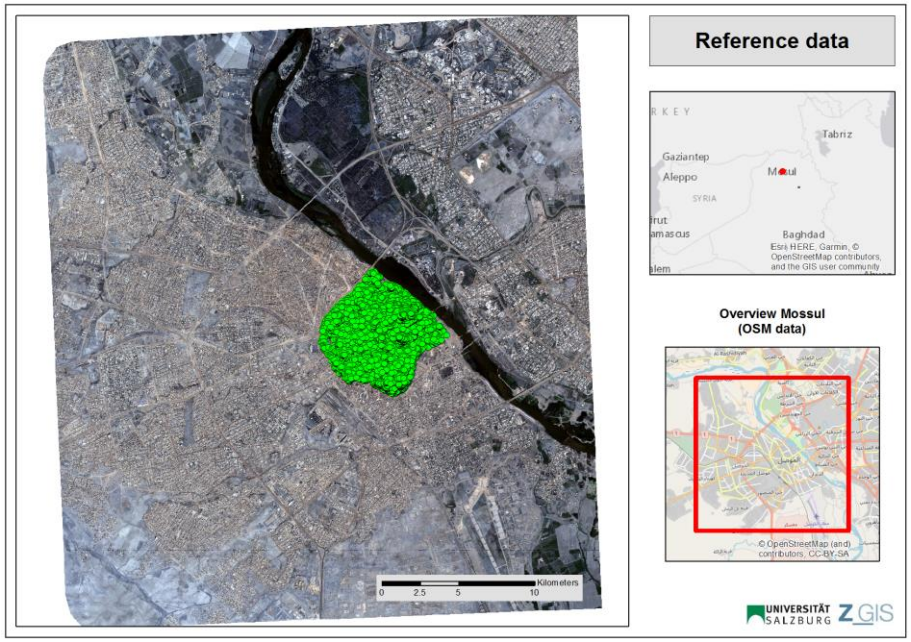

FIGURE 2. Overview about the area covered by the manually mapped reference data from UNOSAT (2017; green point symbols).

3. Methodology

3.1 DSM generation

Digital surface models (DSM) were calculated from the Pléiades images using the fully automatic processing chain CATENA at DLR (Krauß, 2014). CATENA is a multi-purpose, multi-sensor processing environment developed at the Remote Sensing Technology Institute of the German Aerospace Center (DLR). The matching of individual satellite images is based on Semi-Global Matching, SGM (Hirschmuller, 2008). As shown in FIGURE 3, a task is ingested to the task-database telling the system which satellite scene(s) should be processed together with which chain. The distributed processing nodes of the cloud system check regularly the task database for new jobs, fetch them and process these locally on the processing node. The original data will come from a central storage where also the results are stored after successful processing.

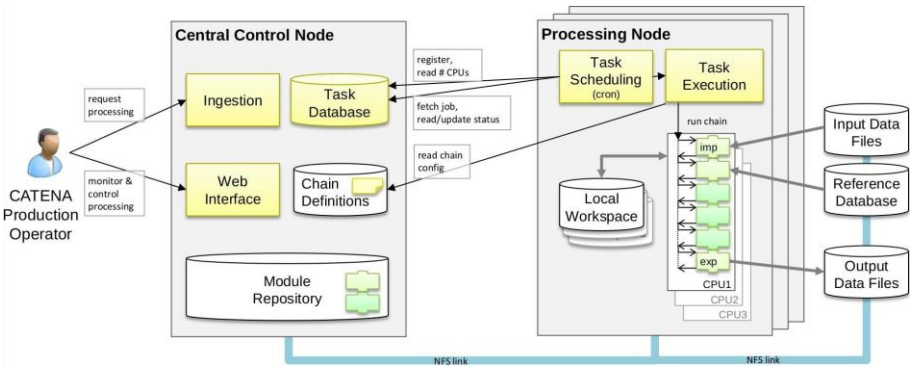

FIGURE 3. Distributed processing environment of CATENA.

CATENA supports many types of original satellite imagery ranging from low resolution like AATSR or MERIS over high resolution like Landsat, Sentinel, IRS, SPOT up to very high resolution (VHR) data like WorldView, GeoEye or Pléiades. All these proprietary input formats are converted during import to a standardized format containing all relevant metadata and can be processed by a permanently growing selection of processing chains containing general tasks like coregistration, orthorectification, cloud-/watermasking or atmospheric correction and various project-specific purposes ranging from forest- and landcover-classification to susceptibility for flooding in strong rain events. One of the most prominent general purpose chains is the multistereo processing chain supporting all VHR stereo satellite scenes. In the project X3D4Pop this chain was extended to also allow the processing of data from different sensors, dates and orbits instead of only the standard in-orbit-(multi)-stereo scenario.

3.2 Object-based 3D damage assessment

An object-based image analysis approach was applied on the 3D elevation data and the 2D images for the damage assessment between the two time steps. Overall, the approach aims at remaining independent from data-specific attributes to allow transferability to other scenes with only very few adaptations. A low error of commission was favored over a lower error of omission, to reach a high reliability for detected damages. This also takes into account, that in both data sets gaps were present, resulting in uncertainties for these areas. Processing has been carried out in the software environment of eCognition Developer (Trimble). In the following, the applied approach will be elaborated in detail.

A vegetation mask was derived for both time steps separately (on different "maps") based on the NDVI, vegetation objects were merged and the 2015 and 2017 vegetation masks were combined in one analysis environment for further analysis.

Both the tri-stereo DSM from 2015 and the cross-stereo DSM from 2017 contain data gaps, in particular in shadowed or occluded areas at the foot of buildings (see FIGURE 4).The data w used without interpolation to ensure conducting the damage assessments on locations with valid data only, gaps were treated as no data areas.

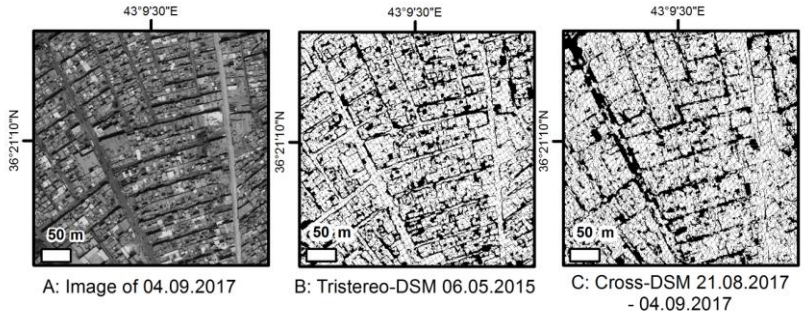

FIGURE 4. Comparison of valid data coverage. Panchromatic satellite image (A), tristereo DSM (B) and cross-stereo DSM (C). Data gaps in the DSMs are depicted in black color.

The classification focused on areas containing height values only. No data values were masked out. To further narrow down the overall number of objects, all potential built-up areas in 2017 were identified. Such objects are contained in 2015 as built up and further have a positive evaluation in 2017 as well.

To identify potentially damaged areas, all objects with a lower elevation in 2017 than in 2015 were classified. Such identified potentially damaged areas were further categorized in three different height classes: changes in height values between of 2015 and 2017 of (i) at least 8 m, (ii) at least 4 m, and (iii) at least 2 m. The minimum value of 2 m was defined to compensate smaller matching errors due to errors contained in the DSM data and 2 m are an approximate height per story.

In a final step, all smaller enclosed objects per class have been assigned to the respective enclosing class. This reduces the noise in the data set and derives a clearer final dataset. Afterwards the classification results were merged, exported and evaluated as described in the subsequent chapter.

4 Results and validation

Results from the classification approach as well as results from the validation are illustrated in FIGURE 5. The classification outcomes are categorized in four different classes: (1) undamaged (built-up) areas in grey, (2) damaged areas with a height difference of 2 m or more in orange, (3) damaged areas with a height difference of 4 m or more in blue, and (4) damaged areas with a height difference of 8 m or more in red. Validation points are indicated as cross symbols in FIGURE 5. From the reference data only points labeled as “destroyed” were selected.

Therefrom, a randomly distributed selection of 120 validation points, i.e. about 10% of the total amount of available reference points were used for the validation. Every single reference point was visually checked to evaluate the classification accuracy. Each cross represents one validation point with indicated damage from the UNOSAT data. Green colored crosses indicate a positive detection of damage in the classification results. Black colored crosses indicate a non-classification, i.e. a manually identified damage was not detected by the classification approach.

Overall, the validation results in a point match of 73 % (87 out of 120 points). The points indicating a non-match are overlaying mostly areas without information (nodata areas). Overlays with built-up areas occur only for four out of 33 points, which equals 12 % (3% of total number of validation points). This suggests that the damage assessment by subtraction of Pléiades-derived DSMs is valid for relatively severely damaged buildings, if the coverage with valid elevation data is sufficient.

TABLE 2. Classification accuracy values and detailed assessment of misclassified points.

		Number	Percentage
Overall Classification Accuracy	Total number of points	120	100 %
	Points located in damaged areas	87	73 %
Detailed assessment of misclassified points	Total number of misclassified points	33	100%
	Built-up areas	4	12%
	Points located in Nodata areas	29	88%

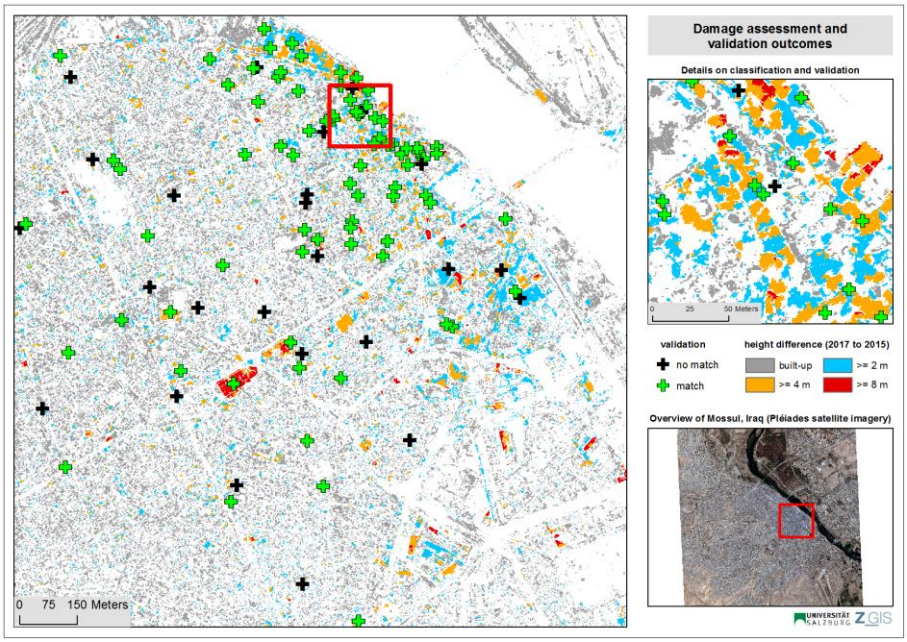

FIGURE 5. Overall classification results and validation outcomes for the damage assessment.

In order to evaluate the used input data, namely the DSM data from 2015 and the DSM data from 2017, the share of nodata areas was calculated. Nodata values represent pixel without height information. This has been carried out for the spatial extent of the available reference data (see FIGURE 2). This area corresponds to a total number of 20,671,200 pixels. The DSM from 2015 contains 7,493,166 pixels with nodata values which equals 36 %. The DSM from 2017 contains 4,907,548 pixels with nodata values which equals 24 %. Combined from 2015 and 2017 all pixels with nodata values amount to 9,229,654 which equals 45 %. The outcomes are illustrated in TABLE 3.

TABLE 3. Evaluation of DSM data sets from 2015 and 2017 for the spatial extent of the reference data.

	Total number of pixels	**Pixels with nodata values**	**Percentage**
DSM of 2015	20671200	7493166	36 %
DSM of 2017	20671200	4907548	24 %
2015 & 2017 combined	20671200	9229654	45 %

5 Discussion and outlook

The proposed approach is a contribution to assess the degree of damage in conflict areas in addition to typical visual assessments on optical image data only. The quality of the derived DSM and the damage assessment depends on the available imagery (time between acquisitions, viewing geometry, sensor mix), but is in any case an additional valuable information source. The usage of mixed-date stereo models increases the likeliness to find suited data shortly after such an event and therefore it strongly supports time-critical damage assessments based on satellite data.

The presented approach is solely based on height information from two different DSM except the vegetation masking based on NDVI values. It therefore illustrates a valid and applicable approach for an initial indication shortly after crisis events.

If absolute building heights are needed, the approach can be extended to derive digital terrain models from the data as presented by Luethje et al., (2017). Especially in urban areas, the generation of a DSM is often limited due to a lack of data coverage induced by shading, too large incident angles, which hinders full coverage with height information. In the presented study, also larger data gaps exist within the two data sets. These gaps occur predominantly in street canyons and shaded areas. Also, the masking of vegetated areas may cause increase these areas in their extent. However, the overall assessment of damage areas is still possible for deriving an indication based on height differences.

As a high quality of the DSM is a crucial requirement for the analysis within the presented approach, a subsequent step will be to evaluate the DSM more profound in the beginning. Such an initial assessment should also indicate if a further damage assessment provides added value with the available datasets. Another point of investigation will be to analyze the amount of data gaps in potentially built up areas compared to nodata pixels in areas that contain vegetation and/or water. Therefore additional, publicly available datasets may be used. Finally, the potential of region growing approaches for the classification results will be investigated to derive objects that correspond better to the footprint of houses. This may also compensate the influence of positional deviations in manually mapped (point) reference datasets.

Overall, the approach aims at a quick, cost-efficient and transferable solution for the support of recovery measures in crisis situations. In the given application domain this is prioritized over very sophisticated but costly (time and money) solutions.

Acknowledgements

This work is part of the research project "Suitability of mixed-sensor derived 3D data for rapid urban population estimation in crisis situations (X3D4Pop)". It is partially funded by the Austrian Research Promotion Agency (FFG) within the Austrian Space Applications Program (ASAP) under grant FFG-ASAP-859796, the Swiss Space Office SSO and the German Aerospace Center DLR.

References

BBC (2017, online). http://www.bbc.com/news/world-middle-east-37702442 [accessed April 2018]

Brunner, D., Lemoine, G., & Bruzzone, L. (2010). Earthquake Damage Assessment of Buildings Using VHR Optical and SAR Imagery. *IEEE Transactions on Geoscience and Remote Sensing*, *48*(5), 2403–2420. https://doi.org/10.1109/TGRS.2009.2038274

Buck, O., Millán, V. E. G., Klink, A., & Pakzad, K. (2014). Using information layers for mapping grassland habitat distribution at local to regional scales. *International Journal of Applied Earth Observation and Geoinformation*, *37*, 83–89. https://doi.org/10.1016/j.jag.2014.10.012

d'Oleire-Oltmanns, S., Eisank, C., Dragut, L., Schrott, L., Marzolff, I., & Blaschke, T. (2012). Object-based landform mapping at multiple scales from digital elevation models (DEMs) and aerial photographs. In *Proceedings of the 4th GEOBIA* (pp. 496–500). Rio de Janeiro, Brazil. Retrieved from http://mtc-m18.sid.inpe.br/col/sid.inpe.br/mtc-m18/2012/05.17.13.40/doc/132.pdf

d'Oleire-Oltmanns, S., Marzolff, I., Peter, K., & Ries, J. (2012). Unmanned Aerial Vehicle (UAV) for Monitoring Soil Erosion in Morocco. *Remote Sensing*, *4*(12), 3390–3416. https://doi.org/10.3390/rs4113390

Erdik, M., Şeşetyan, K., Demircioğlu, M. B., Hancılar, U., & Zülfikar, C. (2011). Rapid earthquake loss assessment after damaging earthquakes. *Soil Dynamics and Earthquake Engineering*, *31*(2), 247–266. https://doi.org/10.1016/j.soildyn.2010.03.009

Hirschmuller, H. (2008). Stereo Processing by Semiglobal Matching and Mutual Information. *IEEE Transactions on Pattern Analysis and Machine Intelligence*, *30*(2), 328–341. https://doi.org/10.1109/TPAMI.2007.1166

Kaiser, A., Neugirg, F., Rock, G., Müller, C., Haas, F., Ries, J., & Schmidt, J. (2014). Small-Scale Surface Reconstruction and Volume Calculation of Soil Erosion in Complex Moroccan Gully Morphology Using Structure from Motion. *Remote Sensing*, *6*(8), 7050–7080. https://doi.org/10.3390/rs6087050

Kosugi, Y., Sakamoto, M., Fukunishi, M., Lu, W., Doihara, T., & Kakumoto, S. (2004). Urban Change Detection Related to Earthquakes Using an Adaptive Nonlinear Mapping of High-Resolution Images. *IEEE Geoscience and Remote Sensing Letters*, *1*(3), 152–156. https://doi.org/10.1109/LGRS.2004.828917

Krauß, T. (2014). Six years operational processing of satellite data using catena at DLR: Experiences and recommendations. *Kartographische Nachrichten*, *64*(2), 74–80.

Levick, S. R., & Rogers, K. H. (2008). Structural biodiversity monitoring in savanna ecosystems: Integrating LiDAR and high resolution imagery through object-based image analysis. *ObjectBased Image Analysis*, 477–491. Retrieved from http://dx.doi.org/10.1007/978-3-540-77058-9_26

Luethje, F., Tiede, D., & Eisank, C. (2017). Terrain Extraction in Built-Up Areas from Satellite Stereo-Imagery-Derived Surface Models: A Stratified Object-Based Approach. *ISPRS International Journal of Geo-Information*, *6*(1), 9. https://doi.org/10.3390/ijgi6010009

Rutzinger, M., Höfle, B., & Pfeifer, N. (2008). Object detection in airborne laser scanning data - an integrative approach on object-based image and point cloud analysis. *Object-Based Image Analysis. Spatial Concepts for Knowledge Driven Remote Sensing Applications*, 817.

Serna, C. G., Pillay, R., & Trémeau, A. (2015). Data Fusion of Objects Using Techniques Such as Laser Scanning, Structured Light and Photogrammetry for Cultural Heritage Applications. In *Computational Color Imaging, Cciw 2015* (Vol. 9016, pp. 208–224). https://doi.org/10.1007/978-3-319-15979-9_20

Stöcker, C., Eltner, A., & Karrasch, P. (2015). Measuring gullies by synergetic application of UAV and close range photogrammetry — A case study from Andalusia, Spain. *CATENA*, *132*, 1–11. https://doi.org/10.1016/j.catena.2015.04.004

Strasser, T., & Lang, S. (2015). Object-based class modelling for multi-scale riparian forest habitat mapping. *International Journal of Applied Earth Observation and Geoinformation*, *37*, 29–37. https://doi.org/10.1016/j.jag.2014.10.002

Symeonakis, E., & Drake, N. (2004). Monitoring desertification and land degradation over sub-Saharan Africa. *International Journal of Remote Sensing*, *25*(3), 573–592. https://doi.org/10.1080/0143116031000095998

Tiede, D., Lang, S., Füreder, P., Hölbling, D., Hoffmann, C., & Zeil, P. (2011). Automated Damage Indication for Rapid Geospatial Reporting. *Photogrammetric Engineering & Remote Sensing*, *77*(9), 933–942. https://doi.org/10.14358/PERS.77.9.933

Vrieling, A., Rodrigues, S. C., Bartholomeus, H., & Sterk, G. (2007). Automatic identification of erosion gullies with ASTER imagery in the Brazilian Cerrados. *International Journal of Remote Sensing*, *28*(12), 2723–2738. https://doi.org/10.1080/01431160600857469

UNOSAT, 2017. http://www.unitar.org/unosat/node/44/2631?utm_source=unosat-unitar&utm_medium=rss&utm_campaign=maps [accessed March 2018]